



## NRC Publications Archive Archives des publications du CNRC

### **Relationship between the spectral line based weight-sum-of-gray-gases model and the full spectrum k-distribution model**

Liu, Fengshan; Chu, Huaqiang; Consalvi, Jean-Louis

This publication could be one of several versions: author's original, accepted manuscript or the publisher's version. /  
La version de cette publication peut être l'une des suivantes : la version prépublication de l'auteur, la version acceptée du manuscrit ou la version de l'éditeur.

#### **Publisher's version / Version de l'éditeur:**

*Proceedings of the 7th International Symposium on Radiative Transfer, 2013-06-08*

#### **NRC Publications Record / Notice d'Archives des publications de CNRC:**

<https://nrc-publications.canada.ca/eng/view/object/?id=42efcc17-03c8-4dec-bdc3-793859a2504c>

<https://publications-cnrc.canada.ca/fra/voir/objet/?id=42efcc17-03c8-4dec-bdc3-793859a2504c>

Access and use of this website and the material on it are subject to the Terms and Conditions set forth at

<https://nrc-publications.canada.ca/eng/copyright>

READ THESE TERMS AND CONDITIONS CAREFULLY BEFORE USING THIS WEBSITE.

L'accès à ce site Web et l'utilisation de son contenu sont assujettis aux conditions présentées dans le site

<https://publications-cnrc.canada.ca/fra/droits>

LISEZ CES CONDITIONS ATTENTIVEMENT AVANT D'UTILISER CE SITE WEB.

**Questions?** Contact the NRC Publications Archive team at

PublicationsArchive-ArchivesPublications@nrc-cnrc.gc.ca. If you wish to email the authors directly, please see the first page of the publication for their contact information.

**Vous avez des questions?** Nous pouvons vous aider. Pour communiquer directement avec un auteur, consultez la première page de la revue dans laquelle son article a été publié afin de trouver ses coordonnées. Si vous n'arrivez pas à les repérer, communiquez avec nous à PublicationsArchive-ArchivesPublications@nrc-cnrc.gc.ca.



National Research  
Council Canada

Conseil national de  
recherches Canada

Canada

# RELATIONSHIP BETWEEN THE SPECTRAL LINE BASED WEIGHTED-SUM-OF-GRAY-GASES MODEL AND THE FULL SPECTRUM K-DISTRIBUTION MODEL

Fengshan Liu<sup>1\*</sup>, Huaqiang Chu<sup>\*\*</sup>, and Jean-Louis Consalvi<sup>\*\*\*</sup>

<sup>\*</sup>Measurement Science and Standards, National Research Council  
Building M-9, 1200 Montreal Road, Ottawa, ON, Canada

<sup>\*\*</sup>Anhui University of Technology, Anhui, China

<sup>\*\*\*</sup>Aix-Marseille Université, IUSTI/ UMR CNRS 7343, 5 rue E. Fermi,  
13453 Marseille Cedex 13, France

## ABSTRACT

The relationship between the spectral line based weighted-sum-of-gray-gases (SLW) model and the full-spectrum  $k$ -distribution (FSK) model in isothermal and homogeneous media is investigated in this paper. The SLW transfer equation can be derived from the FSK transfer equation expressed in the  $k$ -distribution function without approximation. It confirms that the SLW model is equivalent to the FSK model in the  $k$ -distribution function form. The numerical implementation of the SLW relies on a somewhat arbitrary discretization of the absorption cross section where as the FSK model finds the spectrally integrated intensity by integration over the smoothly-varying cumulative- $k$  distribution function using a Gaussian quadrature scheme. The latter is therefore in general more efficient as a fewer number of gray gases is required to achieve a prescribed accuracy. Sample numerical calculations were conducted to demonstrate the different efficiency of these two methods. The FSK model is found more efficient than the SLW model in radiation transfer in H<sub>2</sub>O; however, the two models perform similarly in CO<sub>2</sub>.

**Key words:** Gas radiation; Global models; SLW; FSK

## INTRODUCTION

Thermal radiation plays an important role in heat transfer in various practical high-temperature systems, such as furnaces, engines, and combustors, as well as in fire spread. The main challenges of modelling thermal radiation in gaseous media containing high temperature combustion products are twofold: (1) accurate and efficient solution to the spectral radiative transfer equation (RTE) and

---

<sup>1</sup> Corresponding author: Fengshan.liu@nrc-cnrc.gc.ca.

(2) accurate and efficient modelling of the spectral radiative properties of the combustion products. Significant research efforts have been devoted to real-gas radiative properties since the 1950's.

Remarkable progress in the development of accurate and efficient global non-gray gas radiation methods has been achieved in the last two decades or so. These developments were largely based on the  $k$ -distribution methodology first applied to atmospheric sciences by Arking and Grossman [1]. Several global non-gray gas models have been developed in recent years, which include the spectral line based weight-sum-of-gray-gases (SLW) [2,3], the full-spectrum  $k$ -distribution (FSK) [4,5] model, the absorption distribution function (ADF) model [6,7], and the spectral-line moment-based (SLMB) model [8]. Among these models SLW and FSK are by far the two most popular models for the reasons that they have been extensively developed for gas radiation calculations in non-isothermal and inhomogeneous gas mixtures [3,9,5,10] and their model parameters for CO<sub>2</sub> and H<sub>2</sub>O have been determined by line-by-line calculations. Both models are considered as modern development of the classical weight-sum-of-gray-gases (WSGG) model proposed by Hottel and Sarofim within the framework of the zone method [11]. The connection of the SLW and FSK models to the classical WSGG model has been discussed by Denison and Webb [2] and Modest and Zhang [4].

Although the starting points of derivation, the resultant transfer equations, and the numerical implementations of the SLW and FSK models differ, they are actually closely related to each other as first discussed by Modest [5] and recently by Solovjov and Webb [12]. Modest showed that the SLW RTE can be derived from the FSK RTE by approximating the integration over the cumulative  $k$ -distribution function by a trapezoidal scheme [5]. Consequently, Modest concluded that the SLW is the crudest possible implementation of the FSK method [5]. In a recent paper, Solovjov and Webb [12] showed that in isothermal and homogeneous media the FSK model can be derived from the SLW model in the limit of small absorption cross section increment and the two models are just different forms of the very same equation. Although these studies provided some useful insights into the relationships between the two models, the findings are still incomplete and the relationships between the key quantities in the two models have not been thoroughly explored.

The objective of this study is to offer new insights into the relationship and main differences between the SLW and FSK models by conducting a further analysis of the two models in isothermal and homogeneous media.



## SLW AND FSK MODELS IN ISOTHERMAL AND HOMOGENEOUS MEDIA

### The SLW model

Although detailed derivations of the SLW model have been given originally by Denison and Webb [2] two decades ago and more recently by Solovjov and Webb [12], it is useful to present the key steps in arriving at the RTE and the key variables of the SLW model to facilitate the present discussion. The spectral RTE in an absorbing and emitting medium can be written as

$$\frac{dI_\eta(s)}{ds} = -\kappa_\eta I_\eta + \kappa_\eta I_{b\eta} \quad (1)$$

where  $I_\eta$  is the spectral radiation intensity along a path  $s$ ,  $\eta$  is the wavenumber,  $I_{b\eta}$  is the blackbody spectral radiation intensity,  $\kappa_\eta$  is the spectral absorption coefficient of the medium and is related to the spectral absorption cross section of the absorbing molecule  $C_\eta(T_g)$  through  $\kappa_\eta = NYC_\eta(T_g)$  with  $N$  being the gas molar density,  $Y$  the mole fraction, and  $T_g$  the gas temperature. The high resolution spectral absorption cross section  $C_\eta(T_g)$  can be obtained from a line-by-line (LBL) spectroscopic database. The boundary condition at a diffuse gray wall is written as

$$I_{w\eta} = \epsilon_{w\eta} I_{wb\eta} + (1 - \epsilon_{w\eta}) \frac{1}{\pi} \int_{\hat{\mathbf{n}} \cdot \hat{\mathbf{s}} < 0} I_{w\eta} |\hat{\mathbf{n}} \cdot \hat{\mathbf{s}}| d\Omega \quad (2)$$

where the subscript  $w$  stands for quantities at the wall and  $\epsilon_{w\eta}$  is the wall spectral emissivity. In what follows the discussion will be focused on the transfer equations of the SLW and FSK models, since inclusion of the boundary condition in the discussion does not alter the findings of this study.

An important quantity in the SLW method is the absorption line blackbody distribution function (ALBDF), first introduced by Denson and Webb [2], given as

$$F(C_{abs}, T_b, T_g, Y) = \frac{1}{I_b(T_b)} \sum_i \int_{\Delta\eta_i(C_\eta(T_g) < C_{abs})} I_{b\eta}(T_b) d\eta \quad (3)$$

where  $T_b$  and  $T_g$  are respectively the blackbody temperature and gas temperature and  $I_b$  is the spectrally integrated blackbody intensity. Although not explicitly indicated, the spectral absorption cross section  $C_\eta$  and ALBDF also depend on the total pressure of the medium. In this study the total pressure is restricted to  $p = 1$  atm. A detailed discussion of how the gas and blackbody temperatures affect ALBDF was given by Denison [13]. It is noticed that the gas temperature affects ALBDF through the integration regions, as shown in Fig. 1 (the shaded spectral regions represent the integration regions), which will be discussed later on. ALBDF varies between 0 (for very small values of absorption cross section  $C_{abs}$ ) and 1 (for sufficiently large values of  $C_{abs}$ ).

{Insert Fig. 1 here}

The development of the SLW model starts with representing the high-resolution spectral absorption cross section by a set of discrete values  $C_j$  ( $j = 1, 2, \dots, n$ ) with the help of a set of supplemental cross section  $\tilde{C}_0, \tilde{C}_1, \dots, \tilde{C}_n$  [2,12] as shown in Fig. 1. Because the absorption cross section varies rapidly with the wavenumber over many orders of magnitude, the supplemental cross sections have often been chosen logarithmically equally spaced between the minimum value  $\tilde{C}_0 = C_{\min}$  and the maximum value  $\tilde{C}_n = C_{\max}$  [12], i.e.,

$$\tilde{C}_j = C_{\min} (C_{\max} / C_{\min})^{j/n}, \quad j = 0, 1, \dots, n \quad (4)$$

As shown in Fig. 1, the introduction of the set of supplemental cross section divides the wavenumber into spectral segments  $\Delta\eta_{ij}$  over which the absorption cross section varies between  $\tilde{C}_{j-1}$  and  $\tilde{C}_j$  and the spectral integration of ALBDF is performed as shown in Eq. (3). The minimum and maximum absorption cross sections are chosen in such a way that  $C_{\min}$  is sufficiently small to achieve a good compromise between accuracy and computing time and  $C_{\max}$  is sufficiently large so that it covers the entire range of  $C_\eta$  under typical conditions of combustion applications. The spectral regions where the cross sections are less than  $C_{\min}$  are considered as “windows”, which are represented by a “clear gas” ( $j = 0$ ) and assigned an absorption coefficient of  $k_0 = 0$ . In terms of the terminology of the classical WSGG model, each discrete value  $C_j$ , Fig. 1, represents a gray gas whose absorption cross section can be evaluated as [12]

$$C_j = \sqrt{\tilde{C}_{j-1} \tilde{C}_j} \quad (5)$$

The transfer equation of the SLW model is derived by integration of the spectral RTE, Eq. (1), over all the spectral segments  $\Delta\eta_{ij}$  associated with the  $j$ th gray gas [2,12], as also shown in Fig. 1. The resultant gray gas RTE in isothermal and homogeneous media in the SLW method is given as [2,12]

$$\frac{dI_j}{ds} = -k_j I_j + a_j k_j I_b \quad (6)$$

where  $k_j$  is the absorption coefficient of the  $j$ th gray gas evaluated as  $k_j = NYC_j$ ,  $a_j$  is the weight factor associated with the  $j$ th gray gas and is defined as [2]

$$a_j = \frac{1}{I_b(T_b)} \sum_i \int_{\Delta\eta_{ij}} I_{bj}(T_b) d\eta \quad (7)$$

Using the definition of ALBDF given in Eq. (3), it can be readily shown that

$$a_j = F(\tilde{C}_j, T_b, T_g, Y) - F(\tilde{C}_{j-1}, T_b, T_g, Y) \quad (8)$$

The weight factor of the clear gas is  $a_0 = F(C_{\min}, T_b, T_g, Y)$  [12]. ALBDF can be evaluated from its definition, Eq. (3), along with a spectroscopic database, such as the recently available HITEMP2010 [14]. Such calculations have been recently conducted by Liu et al. [15] and Pearson et al. [16]. The gray gas intensity  $I_j$  consists of contributions from all the spectral segments  $\Delta\eta_{ij}$  in the wavenumber space, i.e.,

$$I_j = \sum_i \int_{\Delta\eta_{ij}} I_\eta d\eta \quad (9)$$

The total (spectrally integrated) radiation intensity is then simply the summation of all the gray gas intensities

$$I = \sum_{j=0}^n I_j \quad (10)$$

To apply the SLW model to gas radiation calculations in an isothermal and homogeneous medium the supplemental absorption cross sections are first selected according to Eq. (4) and the ALBDF as a function of the absorption cross section for the given conditions of the medium is also made available either calculated from its definition and a high-resolution spectroscopic database or from a correlation algorithm [15,16]. Note that in such applications the blackbody temperature is taken at the gas temperature. The absorption coefficient and the weight factor of the  $j$ th gray gas are then calculated from Eqs. (5) and (8). Once the SLW transfer equation, Eq. (6) is solved for the all gray gases considered, the total intensity is found from Eq. (10).

Although the SLW spectral model, Eqs. (4) and (5), outlined above has been the most popular one for its implementation, it is important to point out that other methods have been suggested and employed. One of these alternative SLW spectral models is to construct the SLW model spectrum through error minimization of the total emissivity described by Denison and Webb [2]. Although it has been shown that this approach works quite well for as few as 3 grey gases [2], it is difficult to be extended for multidimensional and/or non-isothermal problems. Solovjov et al. [17] has recently developed the SLW-1 model based on the error minimization approach for constructing the model spectrum for 1D parallel-plate problems. Another method to construct the SLW spectral model is to employ a numerical quadrature scheme, as suggested by Solovjov and Webb [12].

### The FSK model

Unlike the SLW model, whose starting point of development is a discrete representation of the continuous absorption cross section with the help of a set of supplemental cross sections, the FSK



model does not introduce discretization of the gas absorption coefficient in its transfer equation derivation. As shown by Modest and Zhang [4], the FSK model equation can be derived from either the integral form of RTE or directly from the differential form of RTE by reordering it with the help of a Dirac  $\delta$  function. An elaborated derivation of the FSK model from the differential form of RTE was later given by Modest [5]. Here a brief derivation of the FSK model is provided following the work of Modest [5].

To account for the blackbody intensity variation with wavenumber across the spectrum, a blackbody intensity weighted full-spectrum  $k$ -distribution is introduced as [5]

$$f(T_b, T_g, k) = \frac{1}{I_b(T_b)} \int_0^\infty I_{b\eta}(T_b) \delta(k - \kappa_\eta) d\eta \quad (11)$$

where  $\delta$  is the Dirac-delta function,  $\kappa_\eta$  is the gas spectral absorption coefficient, and  $k$  is an arbitrary but specified value of absorption coefficient. A schematic is illustrated in Fig. 2 showing that the same value absorption coefficient  $k$  intersects with the spectral absorption coefficient many times over the entire spectrum. It is noticed that in an isothermal and homogeneous medium the blackbody temperature  $T$  in Eq. (11) is the same as that of the medium. Multiplying a Dirac-delta function  $\delta(k - \kappa_\eta)$  to the spectral RTE, Eq. (1), and then integrating it over the entire spectrum leads to

$$\frac{dI_k}{ds} = k[f(T_b, T_g, k)I_b - kI_k] \quad (12)$$

where

$$I_k = \int_0^\infty I_\eta \delta(k - \kappa_\eta) d\eta \quad (13)$$

is the intensity integrated over all spectral locations where  $\kappa_\eta = k$ . Eq. (12) can be considered as the transfer equation of the FSK model written in terms of the  $k$ -distribution function. The total intensity (integrated over the entire spectrum) is then evaluated as

$$I = \int_0^\infty I_\eta d\eta = \int_0^\infty I_k dk \quad (14)$$

{Insert Fig. 2 here}

As shown by Modest [5], the  $k$ -distribution function  $f(T_b, T_g, k)$  is ill-behaved, i.e., it is not smoothly varying with  $k$ , and it varies over several orders of magnitude. As such, it is difficult to obtain accurate radiation intensity by integrating  $I_k$  over the absorption coefficient space, as expressed in

the second part of Eq. (14). To expedite the evaluation of the total intensity, the cumulative  $k$ -distribution function is introduced as

$$g(T_b, T_g, k) = \int_0^k f(T_b, T_g, k) dk \quad (15)$$

which is a smooth and monotonically increasing function of  $k$  between 0 and 1. It should be pointed that the cumulative  $k$ -distribution function  $g$  in the FSK model is equivalent to ALBDF in the SLW model, even though the former is a function of the absorption coefficient and the latter is a function of the absorption cross section. With a proper conversion of the absorption cross section to absorption coefficient, it can be shown that ALBDF is identical to  $g$ . For isothermal and homogeneous media,  $f(T_b, T_g, k)$  and  $g(T_b, T_g, k)$  are simply expressed as  $f(T, k)$  and  $g(T, k)$ , where  $T$  represents the gas temperature.

Division of Eq. (12) by  $f(T, k)$  results in

$$\frac{dI_g}{ds} = kI_b - kI_g \quad (16)$$

where

$$I_g = \frac{I_k}{f(T, k)} = \frac{\int_0^\infty I_\eta \delta(k - \kappa_\eta) d\eta}{f(T, k)} \quad (17)$$

Based on the definitions of  $I_g$  and  $g$ ,  $I_k dk = I_g dg$ . Hence the total intensity can now be calculated as

$$I = \int_0^\infty I_\eta d_\eta = \int_0^\infty I_k dk = \int_0^1 I_g dg \quad (18)$$

Because the cumulative  $k$ -distribution function  $g$  is a smooth and monotonically increasing function from 0 to 1, the integration of  $I_g$  in the  $g$  space can be conveniently performed using a numerical quadrature scheme. The Gaussian quadrature is one of the popular choices in such calculations. In general, very good accuracy can be achieved using only about 10 quadrature points, i.e.

$$I = \int_0^1 I_g dg \approx \sum_{i=1}^N w_i I_{g_i} \quad (19)$$

where  $N$  is a number of quadrature points,  $w_i$  is the weight parameter with  $\sum_{i=1}^N w_i = 1$ , and  $g_i$  is the quadrature point. In the application of the FSK model to gas radiation calculations in an isothermal and homogeneous medium the  $k$ -distribution function  $f$  and the cumulative  $k$ -distribution function  $g$  at the given conditions (temperature, total pressure, mole fraction) are first calculated from a high-resolution spectroscopic database over a wide range of absorption coefficient  $k$ . A quadrature scheme is then selected to provide a set of  $w_i$  and  $g_i$  parameters. At a given quadrature point  $g_i$ , the corresponding absorption coefficient  $k_i$  is obtained implicitly from Eq. (15). Once  $k_i$  is available, the FSK transfer equation, Eq. (16), is solved. Finally, the total intensity is calculated using Eq. (19).



Equation (16) is known as the transfer equation of the FSK method and is also regarded as a reordered RTE in the smoothly-varying  $g$ -space and the  $g$  function is a reordered wavenumber bounded between 0 and 1 [5]. As pointed out by Modest [5], the FSK method is exact, i.e., Eqs. (12) and (16) are exact without any approximations. The only approximation in this method for isothermal and homogeneous problems is the integration in the  $g$  space using a quadrature scheme, Eq. (19).

### The relationship between FSK and SLW models

Although the relationship between the FSK and SLW models has been previously discussed by Modest [5] and Solovjov and Webb [12], a further analysis of the two models is presented here to gain new insights into their relationship and to better understand the differences in the numerical implementation of the two models. The relationship between the two models can be revealed by deriving the SLW transfer equation from the FSK transfer equation written in terms of the  $k$ -distribution function, i.e., Eq. (12). Based on the definitions of  $I_k$  and  $f(T, k)$  and the properties of the Dirac-delta function, it can be shown that

$$\begin{aligned}
 I_k &= \int_0^\infty I_\eta \delta(k - \kappa_\eta) d\eta \\
 &= \int_0^\infty I_\eta \delta(k - \kappa_\eta) \frac{d\eta}{d\kappa_\eta} d\kappa_\eta \\
 &= \sum_i \left( I_\eta \left| \frac{d\eta}{d\kappa_\eta} \right| \right) \Big|_{\kappa_\eta=k}
 \end{aligned} \tag{20}$$

and

$$\begin{aligned}
 f(T, k) &= \frac{1}{I_b} \int_0^\infty I_{b\eta}(T) \delta(k - \kappa_\eta) d\eta \\
 &= \frac{1}{I_b} \int_0^\infty I_{b\eta}(T) \delta(k - \kappa_\eta) \frac{d\eta}{d\kappa_\eta} d\kappa_\eta \\
 &= \frac{1}{I_b} \sum_i \left( I_{b\eta}(T) \left| \frac{d\eta}{d\kappa_\eta} \right| \right) \Big|_{\kappa_\eta=k}
 \end{aligned} \tag{21}$$

In Eqs. (20) and (21) the summation is over all spectral locations where  $\kappa_\eta = k$ , Fig. 2. Substituting Eqs. (20) and (21) into Eq. (12) one gets

$$\frac{d}{ds} \left[ \sum_i \left( I_\eta \left| \frac{d\eta}{d\kappa_\eta} \right| \right) \Big|_{\kappa_\eta=k} \right] = k \left[ \sum_i \left( I_{b\eta}(T) \left| \frac{d\eta}{d\kappa_\eta} \right| \right) \Big|_{\kappa_\eta=k} \right] - k \left[ \sum_i \left( I_\eta \left| \frac{d\eta}{d\kappa_\eta} \right| \right) \Big|_{\kappa_\eta=k} \right] \tag{22}$$

Writing the derivative terms in the above equation in the finite difference form and then multiplying  $\Delta k$ , which is a small variation to the absorption coefficient  $k$  as shown in Fig. 2, to Eq. (22) leads to

$$\frac{d}{ds} \left[ \sum_i (I_i \Delta \eta) \right]_{k_{\eta}=k} = k \left[ \sum_i (I_{b\eta}(T) \Delta \eta) \right]_{k_{\eta}=k} - k \left[ \sum_i (I_i \Delta \eta) \right]_{k_{\eta}=k} \quad (23)$$

where  $\Delta \eta$  is the wavenumber variation corresponding to the small variation  $\Delta k$  assigned to  $k$ , see Fig. 2. Based on the definitions of  $I_j$  and  $a_j$  given in Eqs. (9) and (7), respectively, it can be readily recognized that Eq. (23) is identical to the transfer equation of the SLW method given in Eq. (6) with

$$I_j = \sum_i \int_{\Delta \eta_{i,j}} I_i d\eta = \sum_i (I_i \Delta \eta) \Big|_{k_{\eta}=k} \quad (24)$$

and

$$a_j = \frac{1}{I_b} \sum_i \int_{\Delta \eta_{i,j}} I_{b\eta}(T) d\eta = \frac{1}{I_b} \sum_i (I_{b\eta}(T) \Delta \eta) \Big|_{k_{\eta}=k} \quad (25)$$

The above derivation of the transfer equation of the SLW model from that of the FSK model written in terms of the  $k$ -distribution function suggests that the SLW model is equivalent to the FSK model expressed in  $I_k$  and the  $k$ -distribution function  $\mathcal{H}(T, k)$ . However, the transfer equation of the FSK model written in  $I_k$  and  $\mathcal{H}(T, k)$  is only its intermediate form, but not the final one expressed in  $I_g$ , though the transfer equation of the SLW model can also be manipulated to arrive at an equivalent form as that for  $I_g$  [12]. The above derivation also establishes the relationships between  $I_k$  and  $I_j$  and  $\mathcal{H}(T, k)$  and  $a_j$  as

$$I_j = I_k \Delta k \quad (26)$$

$$a_j = f(T, k) \Delta k = \Delta g \quad (27)$$

The second part of Eq. (27) is a result of the definition of  $g$  given in Eq. (15). Eqs. (26) and (27) establish the relationships between the quantities in SLW and FSK models.

The above derivation of the SLW transfer equation from the FSK transfer equation written in terms of the  $k$ -distribution function suggests that both the SLW and FSK transfer equations are exact, if the spectral intervals are kept infinitely small in the SLW model, confirming the conclusion of Solovjov and Webb [12]. However, there indeed exist significant differences between the two models in their numerical implementations. In the SLW model, the total intensity is the summation of contributions from all gray gases, Eq. (10). In view of Fig. 1 the total intensity in the SLW model can also be written as

$$I = \sum_{j=0}^n I_j = \sum_j I(C_j) \Delta C_j = \int_0^\infty I(C) dC \quad (28)$$

in the limit of infinitely small absorption cross section divisions. Because the absorption cross section varies over several orders of magnitude, it is difficult to obtain accurate total intensity by integration directly over the absorption cross section space. This implies that it is difficult to design a set of supplemental absorption cross section that is as efficient and accurate as a Gaussian type quadrature scheme as far as total intensity calculation is concerned. However, this is exactly how the SLW model has often been implemented numerically by discretizing the absorption cross section by designing a spectral model as discussed in Section 2.1. On the other hand, the FSK model does not deal with the transfer equation written in terms of  $I_k$  and the  $k$ -distribution function  $f(T, k)$ , Eq. (12), to obtain the total intensity; otherwise, the FSK model would share the same drawback as the SLW model. Instead, the FSK model solves the transfer equation written in  $I_g$  and then evaluates the total intensity according to the last part of Eq. (18) by using a Gaussian type quadrature scheme by taking the advantage that the cumulative function  $g$  is a smoothly-varying function between 0 and 1.

Although the SLW and FSK transfer equations are just different form of the very same equation as shown above and by Solovjov and Webb [12], use of the different forms of the same equation is the fundamental reason for the different numerical implementations of these two methods. As a result of taking the advantage of a Gaussian quadrature scheme in the implementation of FSK method, it is expected that the FSK method is in general more efficient than the SLW method, since it is expected that fewer quadrature points (or gray gases) are needed to achieve the same accuracy. Besides this major difference between SLW and FSK models, another difference between the two models worth pointing out lies in the treatment of the clear gas. In the SLW model, the clear gas is treated explicitly. In the FSK model, however, the clear gas is not considered explicitly.

## RESULTS AND DISCUSSION

The SLW and FSK models were used to calculate radiative heat transfer in one-dimensional isothermal and homogeneous gases between two planar plates containing either  $H_2O$  or  $CO_2$ . The logarithmically equally spaced model spectrum was used for the SLW implementation while the Gauss quadrature scheme was employed for the FSK calculations. These choices are based on the considerations that they have been frequently used in previous studies. In all the calculations of this study the wall surfaces were assumed black and the medium was at a uniform total pressure of 1 atm. Numerical calculations were conducted using the discrete-ordinates method (DOM) by employing 20 uniform grids and the  $T_3$  angular quadrature set with 72 directions in the entire  $4\pi$



solid angle. Further detail about the RTE solver can be found in Chu et al. [18]. The line-by-line (LBL) results were also obtained using the HITTEMP2010 database [14] with details provided in [18]. Although exact solution to the problems at hand exist and there is no need to use DOM to obtain the numerical results, we used DOM in this study mainly for the reasons that the code has been extensively used in our previous studies and DOM is very accurate in 1D plate enclosure. Use of DOM to solve RTE should not alter the findings of this study.

### Model parameters

For calculating radiative heat transfer, we firstly need ALBDF for the SLW model and the  $k$ -distribution and cumulative  $k$ -distribution functions for the FSK model. ALBDF of CO<sub>2</sub> and H<sub>2</sub>O were calculated based on its definition given in Eq. (3) and the HITTEMP2010 database. The  $k$ -distribution function was calculated using the expression given in Eq. (21) and the HITTEMP2010 database. Once the  $k$ -distribution function is available, the cumulative distribution function can be readily calculated from its definition, i.e., by integration of the  $k$ -distribution function, Eq. (15).

{Insert Fig. 3 here}

The ALBDFs of H<sub>2</sub>O at  $T_g = 1000$  K and different blackbody source temperatures and water mole fractions are shown in Fig. 3. Fig. 3(a) shows the ALBDFs of pure H<sub>2</sub>O at five different blackbody temperatures of 500, 1000, 1500, 2000, and 2500 K. Fig. 3(b) shows the effect of self-broadening of H<sub>2</sub>O, which is quite strong and must be taken into account, at two blackbody temperatures of 500 and 1500 K. The ALBDFs of CO<sub>2</sub> at  $T_g = 1000$  K and different blackbody temperatures are shown in Fig. 4. Since the effect of self-broadening of CO<sub>2</sub> is small and can be neglected, these results were calculated for CO<sub>2</sub> mole fraction of 0.5.

{Insert Fig. 4 here}

The  $k$ -distribution functions for H<sub>2</sub>O and CO<sub>2</sub> at  $T_g = 1000$  K are shown in Fig. 5 for two blackbody temperatures of 500 and 1000 K. These results indicate that the  $k$ -distribution function spans over several orders of magnitude and does not vary smoothly with  $k$ , as discussed previously by Modest [5]. To demonstrate the equivalence of ALBDF and the cumulative  $k$ -distribution function  $g$ , the molecular absorption cross section is converted to absorption coefficient using their relationship,

i.e.,  $k = NYC$  with  $Y = 1$ , and the results of ALBDF,  $F$ , and  $g$  are compared directly in Fig. 6. It is evident that they are essentially identical. The very slight differences between  $F$  and  $g$  can be attributed to numerical error, since two different procedures were used in their calculations as mentioned earlier.

{Insert Fig. 5 here}

{Insert Fig. 6 here}

### Radiative transfer in isothermal and homogeneous H<sub>2</sub>O

In this case, the separation distance between the parallel plates is 0.1 m. The medium is pure water vapor at 1000 K. The two walls are black and cold. Fig. 7(a) displays the distributions of the radiative source term calculated by the SLW model using different numbers of gray gases between 3 and 20. It is noted that the SLW results of  $N_{gg} = 3$  are not shown in Fig. 7(a) simply because they are in such large error that they do not fit in the range of values in the figure. Results of the FSK model using different numbers of quadrature points (3 to 12) are shown in Fig. 7(b). Also plotted in Fig. 7 are the LBL results calculated from the HITEMP2010 database. It can be seen from these figures that the accuracy of both SLW and FSK method improves with increasing the number of gray gases or the quadrature points. To quantify the errors of the SLW and FSK results Fig. 8 displays the relative errors calculated as  $(Q_{approx} - Q_{LBL})/Q_{LBL} \times 100\%$ , where  $Q_{approx}$  is the source term calculated from either SLW or FSK model and  $Q_{LBL}$  is the source term from the LBL approach. For the SLW model when the number of gray gases is equal to or greater than 12 a further increase in the number of gray gases does not significantly improve the accuracy of the results, Fig. 8(a). The same observation applies to the results of the FSK model when the number of quadrature points is equal to or greater than 5 in this case, Fig. 8(b). These results clearly indicate that the FSK is more efficient since it requires a fewer number of gray gases to reach a given level of accuracy, as expected from the analysis presented earlier. It is observed from Fig. 8 that there is a systematic discrepancy between the LBL results and those of both SLW and FSK models obtained at a large number of grey gases or quadrature points, which is about 1.5% in the central region of the enclosure. It is believed that this systematic discrepancy is due to the inaccuracy in the calculations of ALBDF or  $g$  for H<sub>2</sub>O shown in Fig. 6(a) and the different spectral ranges in LBL calculations (150 – 9300 cm<sup>-1</sup>) and the ALBDF and  $g$  calculations (0 – 30000 cm<sup>-1</sup>).

Additional calculations were also carried out for a large separation distance of  $L = 1$  m. The relative errors of the SLW and FSK models for different numbers of gray gases or quadrature points (not shown) again indicate that the FSK model is more efficient.

{Insert Fig. 7 here}

{Insert Fig. 8 here}

### **Radiative transfer in isothermal and homogeneous CO<sub>2</sub>**

The separation in this case is  $L = 1$  m. The medium is pure CO<sub>2</sub> at 1000 K and the two walls are again black and cold. Results of the SLW and FSK models for different numbers of gray gases or quadrature points are compared with the LBL results in Figs. 9(a) and 9(b), respectively. The corresponding relative errors of the SLW and FSK results are shown in Fig. 10.

{Insert Fig. 9 here}

{Insert Fig. 10 here}

It is interesting to observe from Figs. 9 and 10 that the SLW model performs similar to the FSK model in terms of the accuracy. In fact, the SLW model is slightly more accurate than the FSK model for a given number of gray gases. The reasons for the slightly better performance of the SLW model than the FSK model in the calculation of radiation transfer in CO<sub>2</sub> lie in the different spectral structures of CO<sub>2</sub> and H<sub>2</sub>O absorption coefficient and how the SLW and FSK models handle the ‘clear’ gas. H<sub>2</sub>O absorbs in the entire infrared spectrum, while CO<sub>2</sub> absorbs in four distinct spectral bands. Consequently, CO<sub>2</sub> has appreciable spectral regions where it is almost transparent, which is also revealed in the different behavior of the  $F$  or  $g$  function of H<sub>2</sub>O and CO<sub>2</sub> shown in Fig. 6. Because the SLW model deals with the ‘clear’ gas explicitly, which is more important in radiation transfer in CO<sub>2</sub> than in H<sub>2</sub>O, this is why it performs well in terms of accuracy in radiation transfer calculations in CO<sub>2</sub>. Another way to understand the relative performance of the SLW model and the FSK model shown in Figs. 9 and 10 is to examine the efficiency of a Gauss quadrature. As shown in Fig. 6(b) where  $g$  values less than about 0.25 at  $T_g = T_b = 1000$  K correspond to very small values of absorption coefficients, which contribute negligibly to the total radiation intensity. In this situation, a Gauss quadrature scheme in the FSK model does not offer the same advantage over the



integration over the absorption cross section space along with an explicit treatment of the clear gas as for radiation transfer problems in  $\text{H}_2\text{O}$ .

## CONCLUSIONS

It is shown in this study that the SLW model is equivalent to the FSK model expressed in terms of the full-spectrum k-distribution, but not the RTE in the FSK model expressed in the cumulative k-distribution function. Although the cumulative k-distribution in the FSK model is equivalent to the absorption line blackbody distribution function associated with the SLW model, the two models use these two quantities in a different way. In the SLW model, ALBDF is used to evaluate the weighting factor and the total intensity is obtained by integration over the absorption cross section. On the other hand, the cumulative k-distribution function is used in the FSK method to evaluate the total intensity through a Gaussian type quadrature scheme, which offers high accuracy with relatively few quadrature points, and to implicitly determine the absorption coefficient. As a result of using a Gaussian type quadrature scheme to perform numerical integrations, the FSK model is in general more efficient than the SLW model to achieve a given level of accuracy when implemented numerically. This is indeed the case for radiation transfer in  $\text{H}_2\text{O}$ . In problems containing  $\text{CO}_2$  only, however, the two models perform very similar. The similar performance of SLW to FSK in radiation transfer calculations in  $\text{CO}_2$  can be attributed to the explicit treatment of ‘clear gas’ in the SLW model.

## Acknowledgments

Dr. Huangqiang Chu would like to acknowledge the financial support from the National Major Scientific Instruments Development Project of China (No.2012YQ220119).

## REFERENCES

1. Arking A, Grossman K. The influence of line shape and band structure on temperatures in planetary atmospheres. *J. Atmospheric Sci.* 1972; 29:937-949.

2. Denison MK, Webb BW. A spectral line-based weighted-sum-of-gray-gases model for arbitrary RTE solvers. *ASME J. Heat Transfer* 1993; 115:1004-1012.
3. Denison MK, Webb BW. The spectral line-based weighted-sum-of-gray-gases model in nonisothermal nonhomogeneous media. *ASME J. Heat Transfer* 1995; 117:359-365.
4. Modest MF, Zhang H. The full-spectrum correlated-k distribution for thermal radiation from molecular gas-particulate mixtures. *ASME J. Heat Transfer* 2002; 124:30-38.
5. Modest MF. *Radiative Heat Transfer*, 2<sup>nd</sup> ed., Academic, New York, 2003.
6. Pierrot L, Soufiani A, Taine J. Accuracy of narrow-band and global models for radiative transfer in H<sub>2</sub>O, CO<sub>2</sub>, and H<sub>2</sub>O-CO<sub>2</sub> mixtures at high temperature. *JQSRT* 1999; 62:523-548.
7. Pierrot L, Rivière P, Soufiani A, Taine J. A fictitious-gas-based absorption distribution function global model for radiative transfer in hot gases. *JQSRT* 1999; 62:609-624.
8. André F, Vaillon R. The spectral-line moment-based (SLMB) modeling of the wide band and global blackbody-weighted transmission function and cumulative distribution function of the absorption coefficient in uniform gaseous media. *JQSRT* 2008; 109:2401-2416.
9. Solovjov VP, Webb BW. Application of CW local correction approach to SLW modeling of radiative transfer in non-isothermal gaseous media. *JQSRT* 2010; 111:318-324.
10. Modest MF. Narrow-band and full-spectrum k-distributions for radiative heat transfer – correlated-k vs. scaling approximation. *JQSRT* 2003; 76:69-83.
11. Hottel HC, Sarofim AF. *Radiative Transfer*, McGraw-Hill, 1967.
12. Solovjov VP, Webb BW. Global spectral methods in gas radiation: the exact limit of the SLW model and its relationship to the ADF and FSK methods. *ASME J. Heat Transfer* 2011; 133:042701-1/042701-9.
13. Denison MK. A Spectral Line-based Weighted-Sum-of-Gray-Gases Model for Arbitrary RTE Solvers. Ph.D Thesis, Brigham Young University, USA, 1994.
14. Rothman LS, Gordon IE, Barber RJ, Dothe H, Gamache RR, Goldman A, Perevalov VI, Tashkun SA, Tennyson J. HITEMP, the high-temperature molecular spectroscopic database. *JQSRT* 2010; 111:2139-2150.
15. Liu F, Chu H, Zhou H, Smallwood GJ. Evaluation of the absorption line blackbody distribution function of CO<sub>2</sub> and H<sub>2</sub>O using the proper orthogonal decomposition and hyperbolic correlations. *JQSRT*, available online, 2012.
16. Pearson JT, Webb BW, Solovjov VP, Ma J. Updated correlation of the absorption line blackbody distribution function for H<sub>2</sub>O based on the HITEMP2010 database. *JQSRT*, available online, 2012.
17. Solovjov VP, Lemonnier D, Webb BW. The SLW-1 model for efficient prediction of radiative transfer in high temperature gases. *JQSRT* 2011; 112:1205-1212.

18. Chu H, Liu F, Zhou H. Calculations of gas thermal radiation transfer in one-dimensional planar enclosure using LBL and SNB models. *Int. J. Heat Mass Transfer* 2011; 54:4736-4745.



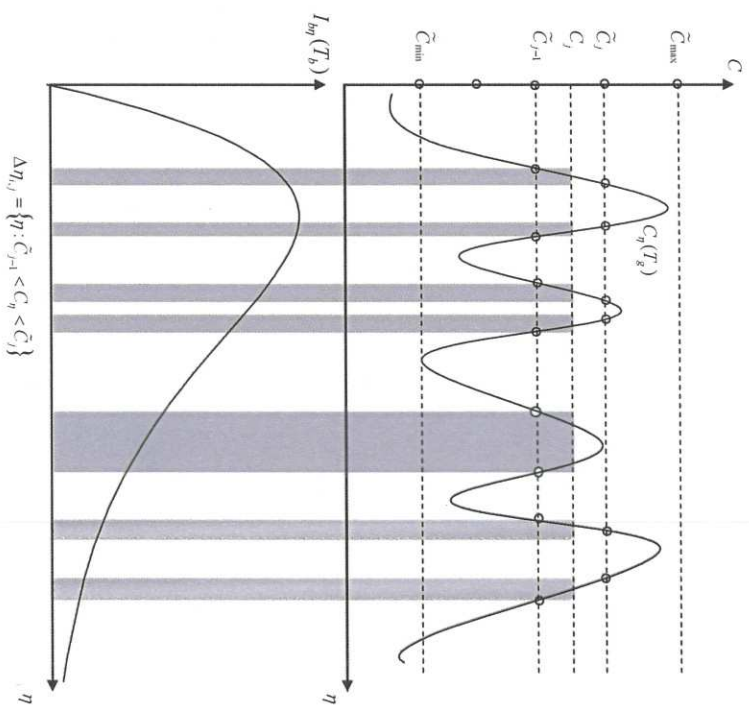


Figure 1. Schematic showing the discretization of the absorption cross section and the corresponding wavenumber intervals of the SLW model.

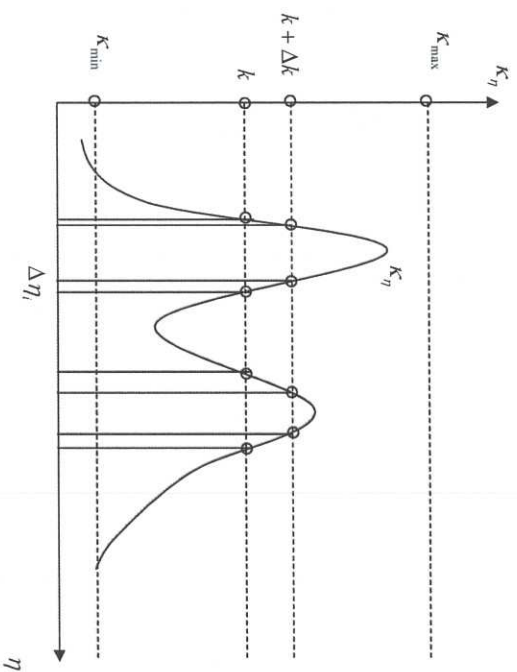


Figure 2. Schematic showing the multiple intersection spectral locations for an arbitrary absorption coefficient  $k$  and the spectral intervals corresponding to a small variation of  $k$ .

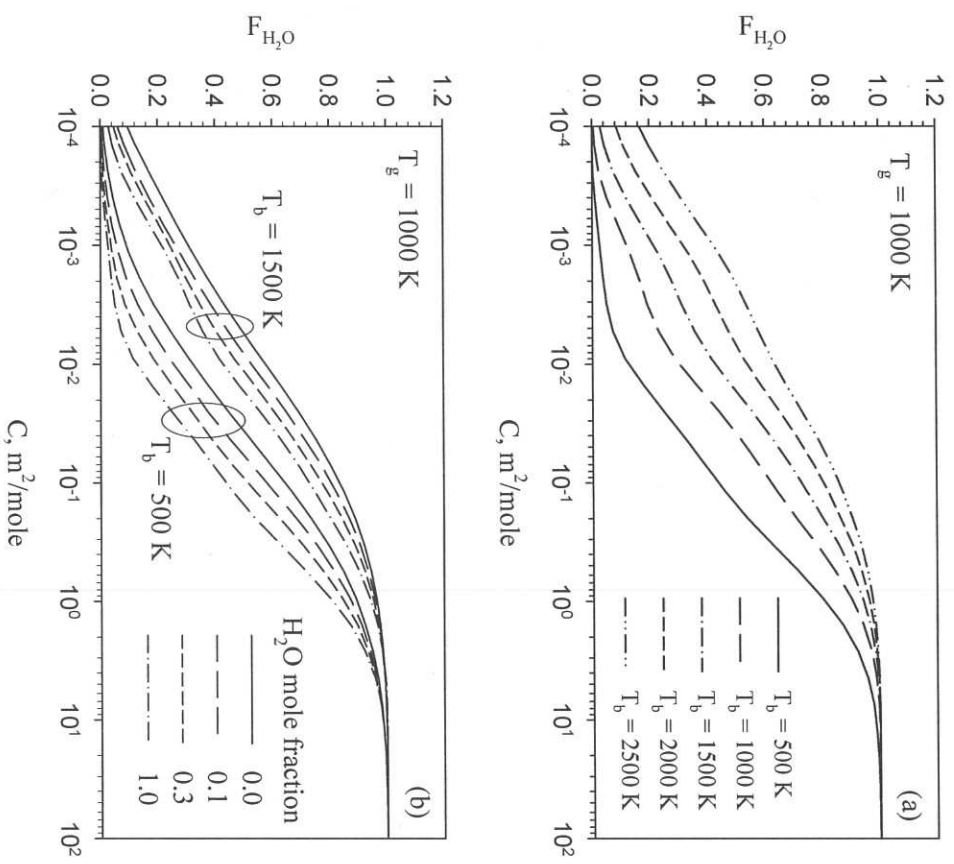


Figure 3. Variations of ALBDF of  $H_2O$  with the blackbody temperature and mole fraction at  $T_g = 1000$  K.



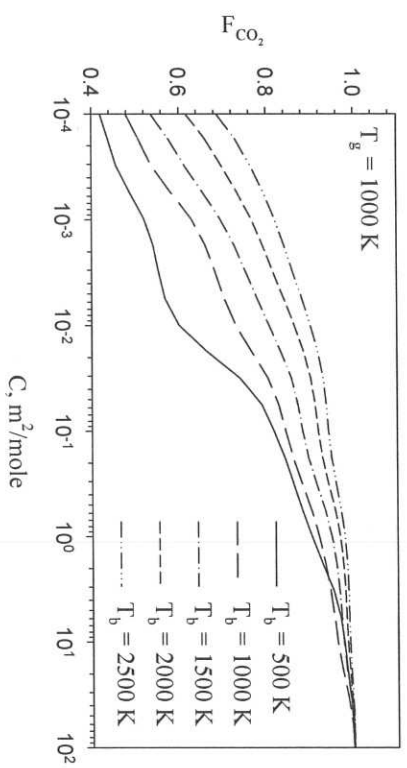


Figure 4 Variations of ALBDF of  $\text{CO}_2$  with the blackbody temperature at  $T_g = 1000 \text{ K}$ .

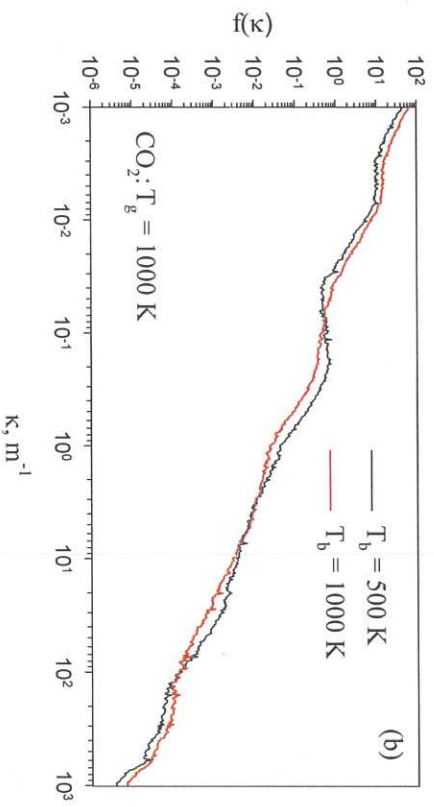
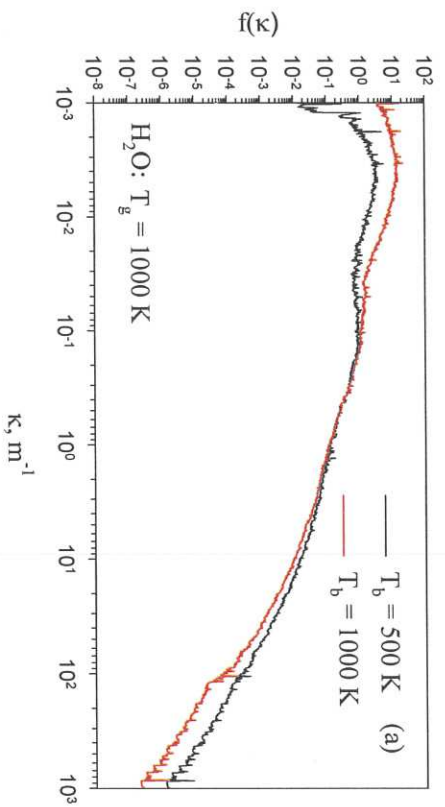


Figure 5. The  $k$ -distribution functions of  $\text{H}_2\text{O}$  and  $\text{CO}_2$  at  $T_g = 1000 \text{ K}$  and  $T_b = 500$  and  $1000 \text{ K}$ .

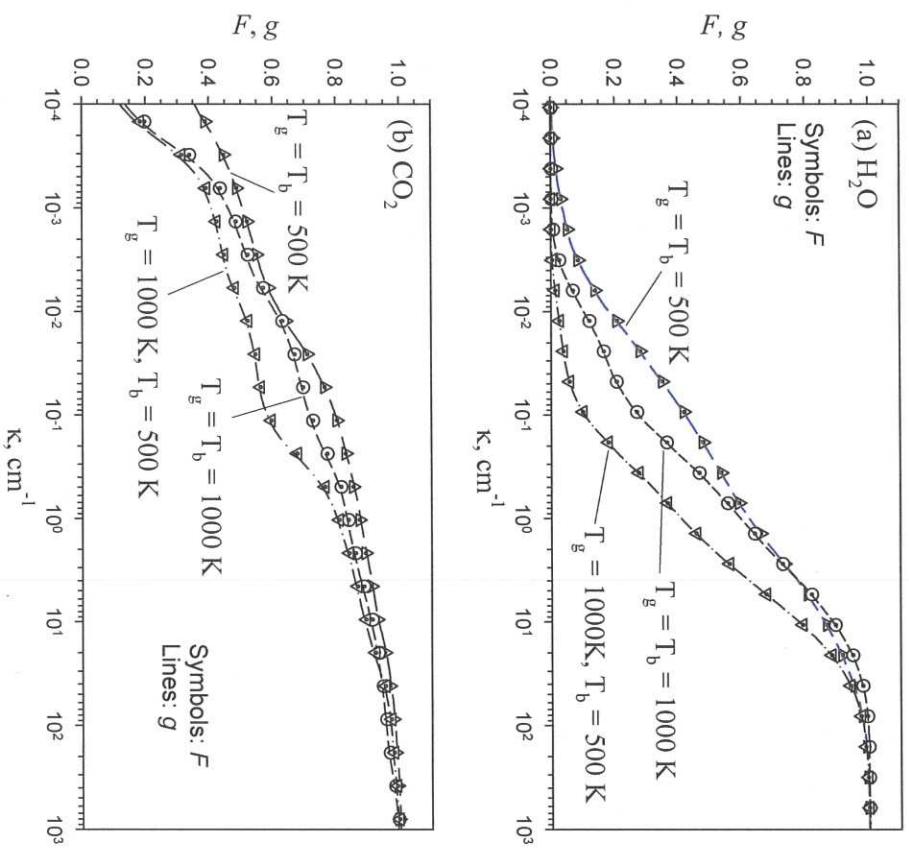


Figure 6. Comparisons of  $F$  and  $g$  of pure  $\text{H}_2\text{O}$  and  $\text{CO}_2$  at three pairs of  $T_g$  and  $T_b$ .



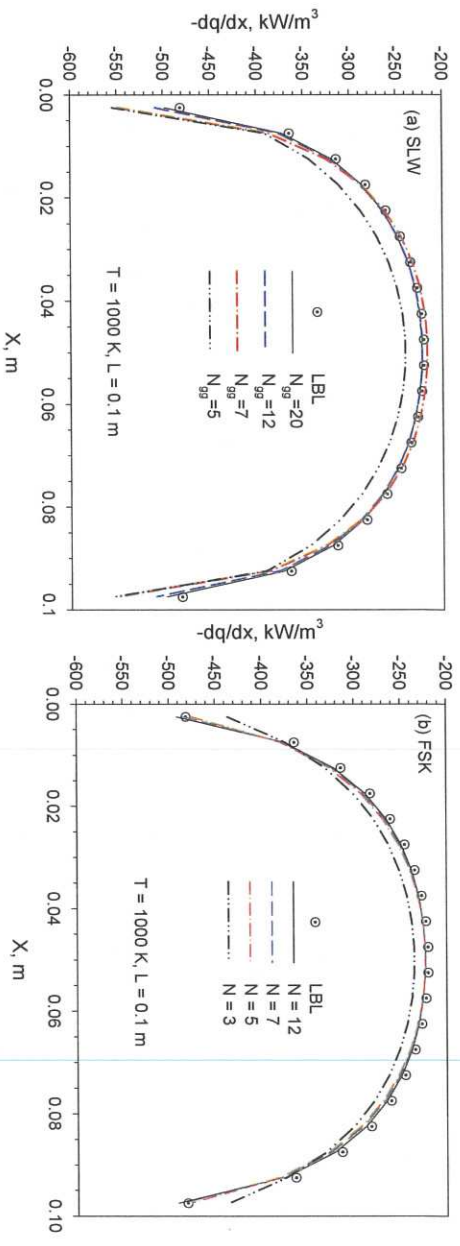


Figure 7. Comparisons of the SLW and FSK results using different numbers of gray gases with the LBL results in  $\text{H}_2\text{O}$ :  $T_g = 1000 \text{ K}$ ,  $L = 0.1 \text{ m}$ .

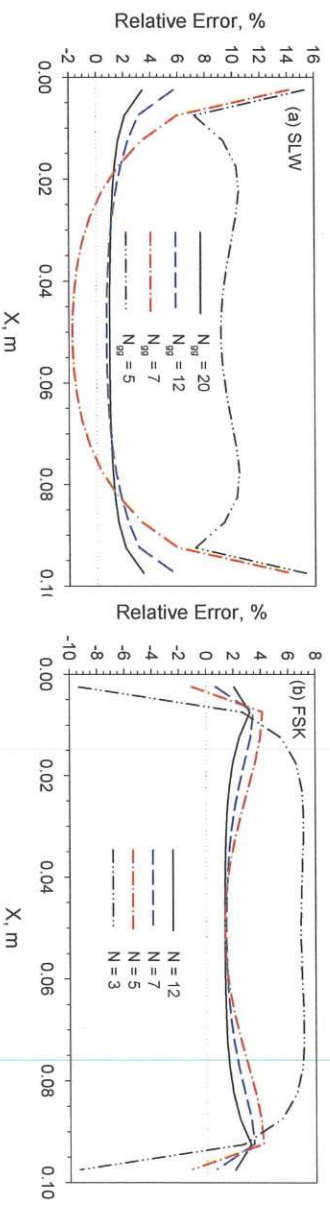


Figure 8. Variation of relative error in the radiative source term with the number of gray gases in the SLW model or the number of quadrature points in the FSK model in  $\text{H}_2\text{O}$ :  $T_g = 1000 \text{ K}$ ,  $L = 0.1 \text{ m}$ .

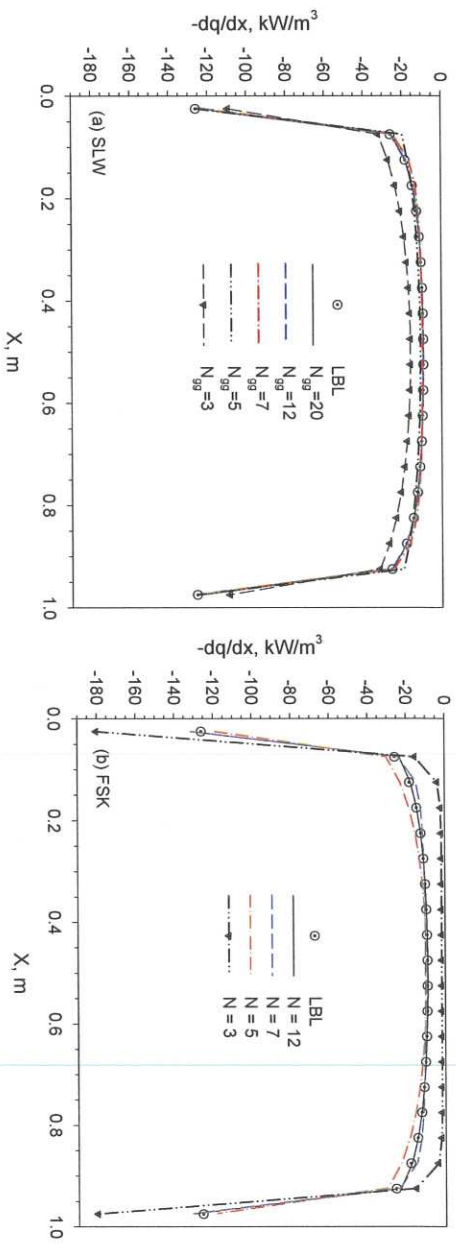


Figure 9. Comparisons of the SLW and FSK results using different numbers of gray gases  
with the LBL results in CO<sub>2</sub>;  $T_g = 1000$  K,  $L = 1$  m.

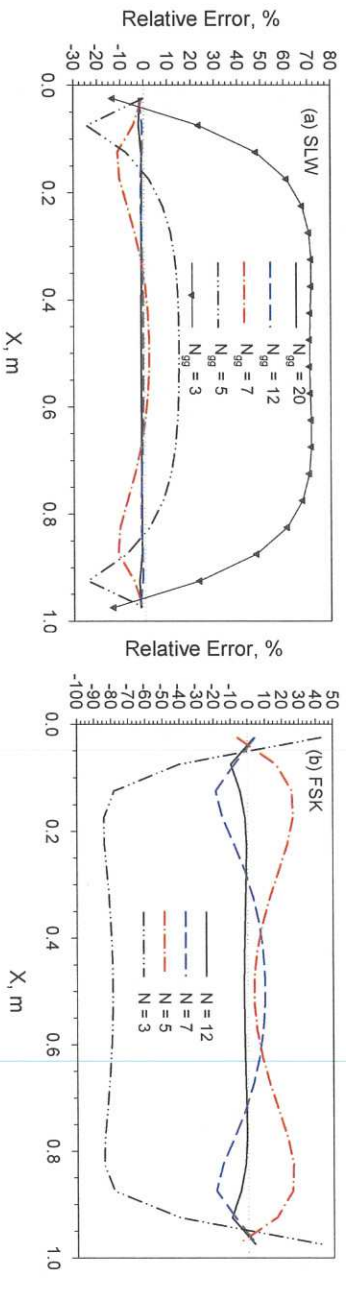


Figure 10. Variation of relative error in the radiative source term with the number of gray gases in the SLW model or the number of quadrature points in the FSK model in CO<sub>2</sub>:  
 $T_g = 1000$  K,  $L = 1$  m.